A Lightweight QRS Detector for Single Lead ECG Signals using a Max-Min Difference Algorithm

Diptangshu Pandit[1], Li Zhang[1], Chengyu Liu[2], Samiran Chattopadhyay[3], Nauman Aslam[1] and Chee Peng Lim[4]

[1]Computational Intelligence Research Group
Department of Computing Science and Digital Technologies
Faculty of Engineering and Environment
University of Northumbria
Newcastle, NE1 8ST, UK

[2]Institute of Biomedical Engineering
School of Control Science and Engineering
Shandong University
Jinan, China

[3]Department of Information Technology
Jadavpur University
Kolkata, India

[4]Institute for Intelligent Systems Research and Innovation
Deakin University
Waurn Ponds, VIC 3216, Australia

Abstract

Background and Objectives: Detection of the R-peak pertaining to the QRS complex of an ECG signal plays an important role for the diagnosis of a patient's heart condition. To accurately identify the QRS locations from the acquired raw ECG signals, we need to handle a number of challenges, which include noise, baseline wander, varying peak amplitudes, and signal abnormality. This research aims to address these challenges by developing an efficient lightweight algorithm for QRS (i.e., R-peak) detection from raw ECG signals.

Methods: A lightweight real-time sliding window-based Max-Min Difference (MMD) algorithm for QRS detection from Lead II ECG signals is proposed. Targeting to achieve the best trade-off between computational efficiency and detection accuracy, the proposed algorithm consists of five key steps for QRS detection, namely, baseline correction, MMD curve generation, dynamic threshold computation, R-peak detection, and error correction. Five annotated databases from Physionet are used for evaluating the proposed algorithm in R-peak detection. Integrated with a feature extraction technique and a neural network classifier, the proposed ORS detection algorithm has also been extended to undertake normal and abnormal heartbeat detection from ECG signals.

Results: The proposed algorithm exhibits a high degree of robustness in QRS detection and achieves an average sensitivity of 99.62% and an average positive predictivity of 99.67%. Its performance compares favorably with those from the existing state-of-the-art models reported in the literature. In regards to normal and abnormal heartbeat detection, the proposed QRS detection algorithm in combination with the feature extraction technique and neural network classifier achieves an overall accuracy rate of 93.44% based on an empirical evaluation using the MIT-BIH Arrhythmia data set with 10-fold cross validation.

Conclusions: In comparison with other related studies, the proposed algorithm offers a lightweight adaptive alternative for R-peak detection with good computational efficiency. The empirical results indicate that it not only yields a high accuracy rate in QRS detection, but also exhibits efficient computational complexity at the order of $O(n)$, where n is the length of an ECG signal.

Keywords: QRS or R-peak detection, feature extraction, ECG analysis, and Max-Min Difference algorithm.

1. Introduction

Electrocardiogram (ECG) represents the myocardial electrical activities of the heart. ECG signals play a significant role in the diagnosis of cardiovascular diseases, such as cardiac arrhythmias, hypertension or ischaemic heart diseases. ECG recordings used to be a time consuming process, and require the examination by on-site cardiologists to detect and diagnose various heart conditions. Nowadays, mobile ECG sensors, such as the Shimmer or Alivecor® sensors [1], are available. These sensors not only are easy to use, but also are affordable and efficient in acquiring ECG readings. However, these ECG mobile sensors predominantly use only 1 or 2 leads (generally Lead I or Lead II) for ECG recording, instead of using all standard 12 leads. Therefore, real-time detection of the QRS positions and abnormality analysis pose a challenging task.

Moreover, interpreting the QRS complex is one of the most important elements in ECG signal processing. In particular, the R wave of the QRS complex plays a vital role for diagnosing heart rhythm irregularities as well as identifying heart rate variability. However, signal abnormality poses another challenge for QRS detection, since the QRS patterns from abnormal ECG signals could be extremely irregular. As an example, an ideal Lead II ECG signal usually consists of P, Q, R, S, and T waves. Fig. 1 shows some examples of real-world raw Lead II ECG samples from the MIT-BIH Arrhythmia database [2]. As can be seen clearly in Fig. 1, even the normal patterns (i.e., a, b, and c signals in Fig. 1) exhibit differences because the ECG signals could be influenced by each individual's physiological condition. Furthermore, the abnormal patterns (i.e., d, e, and f signals in Fig. 1) are hardly comparable with the ideal waveforms, since some of the waves could be missing (e.g. the R wave is

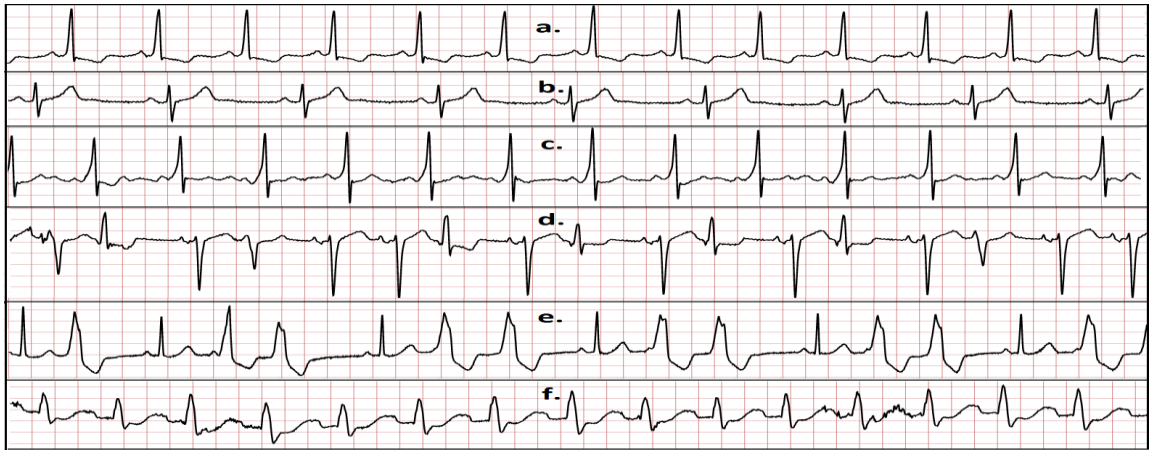

Fig. 1 - Normal (a, b, and c) and abnormal (d, e and f) real ECG signals

missing resulting in an QS wave in signal d.). On the other hand, other waves with high amplitudes (e.g. the T wave) could be mis-identified as the R wave or an QRS pattern.

Fig. 2 (a) shows some detailed normal and abnormal QRS patterns taken from the MIT-BIH Arrhythmia database. These QRS patterns look completely different from one to another, and they tend to confuse state-of-the-art QRS detection algorithms. We have observed that in most cases, the differences in terms of amplitudes pertaining to either QR/RS waves or ST waves indicate the most dramatic change in every QRS complex. Fig. 2 (b) shows the corresponding marked regions of the waves illustrated in Fig. 2 (a). These regions represent the difference between the highest and lowest amplitudes in the corresponding QRS complex.

In view of the aforementioned challenges, this research aims to accurately identify the location of the R wave (if present) from raw ECG signals by exploiting those features illustrated in Fig. 2 (b) to deal with signal abnormality.

Specifically, we propose a sliding window-based Max-Min Difference (MMD) algorithm for robust real-time QRS or R-peak detection from raw single lead (Lead II) ECG signals. In comparison with other R-peak detection algorithms, the proposed MMD algorithm possesses a low computational cost. The proposed algorithm employs a dynamic thresholding method along with an MMD curve generation method for QRS pattern detection. This R-peak detection algorithm is evaluated with ECG signals extracted from multiple databases including the MIT-BIH Arrhythmia [2], European ST-T [3], MIT-BIH ST Change [4], St.-Petersburg Institute of Cardiological Technics 12-lead Arrhythmia [5], and QT [6] databases. To ascertain the efficiency in abnormality detection, the proposed algorithm is combined with a feature extraction technique and a neural

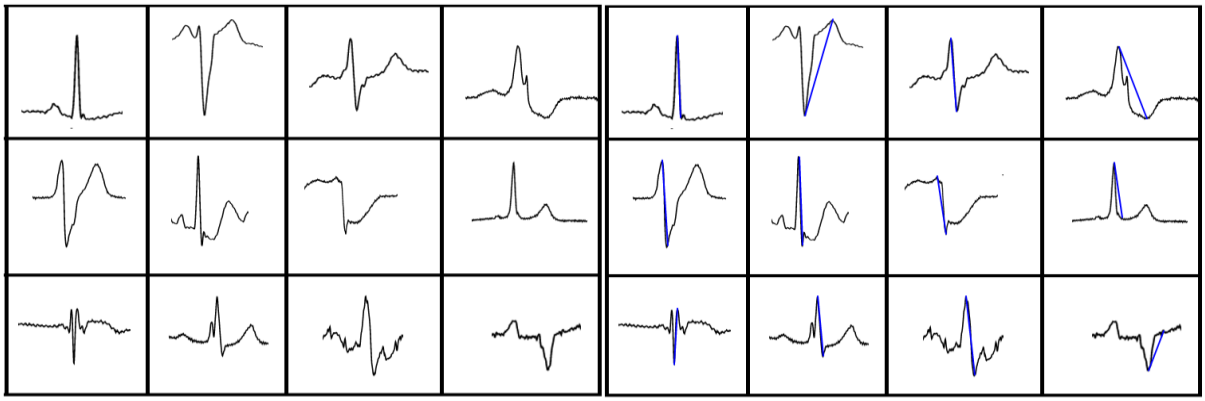

Fig. 2 - (a) Series of heterogeneous QRS patterns, (b) series of heterogeneous QRS patterns, with the highest regional differences of amplitudes marked

network classifier to perform abnormal heartbeat detection using ECG signals from the MIT-BIH Arrhythmia database.

The contributions of this research are summarised as follows. (1) A sliding window-based strategy is employed for online real-time ECG analysis. Instead of requiring the whole signal to be stored in memory, it works sufficiently well with a small buffer of the signal, in order to have a low computational cost. (2) A novel algorithm, i.e., MMD, is proposed for robust QRS detection. The MMD algorithm computes the difference between the local minimum and maximum of a small window and slides it along an ECG signal to find the QRS complex locations. In comparison with related studies, it has a better trade-off between speed and accuracy, and it produces impressive results with a high degree of computational simplicity. (3) Dynamic thresholding is proposed to deal with the problem of fluctuating average peak amplitudes in ECG signals. It calculates the thresholds by using the current peak location, a few previous QRS locations, and the distances in between. (4) The proposed MMD algorithm is evaluated with five ECG databases for QRS detection. In particular, a comprehensive evaluation is conducted using the well-known MIT-BIH Arrhythmia database, and the results are compared with those from other state-of-the-art algorithms for R-peak detection. In order to further ascertain the usefulness of the proposed MMD algorithm, we also perform abnormal/normal heartbeat detection based on the QRS detection by incorporating a feature extraction technique and a neural network classifier. Overall, the empirical results indicate the superiority of the proposed MMD algorithm over other methods in terms of performance and computational cost.

2. Related Work

Computerised ECG analysis has been widely studied, and many advanced methods for QRS detection exist in the literature. Wavelet transform (WT) methods have been used in ECG feature extraction along with other enhancements [7–10]. Other techniques include Geometric Analysis [11], Difference Operation Method [12], Spectral Analysis [13], Cumulative Sums of Squares [14], and Principal Component Analysis [15]. However, the majority of these highly accurate QRS detection algorithms employ complex methods, which require complex time-frequency domain conversion, e.g. Fourier/Wavelet transform, and complex filtering. Such methods require high computational costs and memory resources, which hinder their real-time deployment, especially when the computing resources are limited, e.g. running on tablets or mobile devices. As an example, the computational complexity of Fourier [16] and Wavelet transforms [17–20] depends heavily on the number of segmentations per signal. Increasing the number of segmentations improves signal detection accuracy, at the expense of a high computational cost. The finite impulse response filters involve a large number of multiplication operations, which in turn results in high computational complexity. Hilbert transform [8, 21, 22] comprises costly fast Fourier transform, which also makes it computationally inefficient as compared with time domain methods.

To address computational complexity problems, Elgendi *et al*. [23] presented a thorough revision on the QRS detection methodologies for portable, wearable, battery operated, and wireless ECG devices. A variety of techniques of QRS detection from raw ECG signals were presented in their studies, including thresholding, syntactic methods [24–26], Hidden Markov Models [27], neural networks [28–31], template matching [32], matched filters [28, 33], singularity techniques [34] and zero-crossing [35]. According to Elgendi *et al*. [23], thresholding methods appear to be the most computationally efficient for QRS detection using portable battery

operated devices. However, the empirical results indicate that the initial parameter setting for the thresholding methods is very important in determining the performances [23].

A number of promising solutions such as lightweight QRS detection methods have also been proposed in recent years to address the problem associated with a high computational cost of traditional methods. Adeluyi and Lee [36] proposed a lightweight algorithm for R-peak detection from ECG signals. Known as R-READER, the system relied on the slopes between two neighbourhood signals to identify the R-peak location. Comparing with other well-known QRS detection algorithms, such as Pan and Tompkin [37], the system was able to achieve 96.614% accuracy based on extreme ECG signals from the MIT-BIH Arrhythmia database, and outperformed other related methods with a low computational cost. Chiarugi *et al*. [38] presented another R-peak detection algorithm combining the bandpass filter with both the first derivative and multiple thresholds. Christov [39] used multiple moving window averages along with the first derivative and multiple thresholds for QRS detection, and achieved high numerical efficiency. Elgendi [40] proposed an QRS detection algorithm that incorporated the bandpass filter and the first derivative with squaring. The study employed thresholding with two moving window averages for QRS detection. Wang *et al*. [12] proposed a lightweight algorithm for QRS detection and subsequent feature extraction. Their work used the bandpass filter, difference operation method, and thresholding. Note that the majority of the aforementioned lightweight methods are designed to work on the entire ECG signal, as opposed to window-based processing where only a small portion of the signal is stored for processing. Therefore, in this research, we aim to address this gap by proposing a lightweight window-based method for real-time QRS detection.

On the other hand, wearable energy-efficient ECG monitoring systems have become popular in recent years. Miao *et al*. [41] proposed a wearable context-aware ECG monitoring system integrated with built-in kinematic sensors of a smartphone for physical activity recognition and automatic arrhythmias detection. Their work employed the built-in kinetic sensors of the smartphone to identify users' physical activities. Such context information was exploited to assist the diagnosis of arrhythmias and identification of common abnormal ECG patterns in different activities. Rehman *et al*. [42] conducted a survey on different types of wearable sensors. They discussed the design of ECG and blood pressure wearable sensors, and compared different types of filters for noise (e.g. baseline wander noise, muscle noise) removal from raw ECG signals. Wang *et al*. [43] presented a health monitoring system using wearable wireless ECG sensors with dynamic transmission power control. They employed 3-Lead electrode placements to identify the best electrode positions. A sensor node was deployed to transmit the ECG signals to other devices. To dynamically adjust the transmission power of the sensor node and to save energy consumption, a dynamic power adjustment method was proposed [42]. The outcome indicated the efficiency of the method in reducing power consumption for activity monitoring.

3. Material and Methods

In this section, we introduce the proposed MMD algorithm for QRS detection, as well as for abnormality detection in combination with a feature extraction technique and a neural network classifier.

3.1. QRS Peak Detection

There are a number of challenges encountered when detecting QRS or R-peak locations. These include noise, baseline wander, varying thresholds, and signal abnormality. In this research, the corresponding strategies to solve the abovementioned challenges are discussed, as follows.

- Firstly, to deal with noise embedded in ECG signals, we use sliding window averaging to smooth the signals for QRS detection and analysis, instead of using any bandpass filtering methods. Although this process scales down all the peaks, it does not affect the detection rate of the QRS patterns. The sliding window average method not only is effective in terms of accuracy, but also is efficient in terms of computational cost.
- Secondly, rapid changes in the baseline of the ECG signal, i.e., baseline wander (see Fig. 4), can have a negative impact on the overall detection accuracy. To overcome this problem, we use a simple baseline correction algorithm that involves window-based averaging and deducts the local average of the signal from the raw signal.
- Thirdly, finding an optimal threshold for peak detection is challenging because the amplitude difference between R wave and P or T waves varies not only for signals collected from different subjects but also for those gathered from the same subjects. As a result, dynamic thresholding is proposed in this research to identify the appropriate thresholds, i.e., the minimum value that is above all P or T waves, in diverse cases.

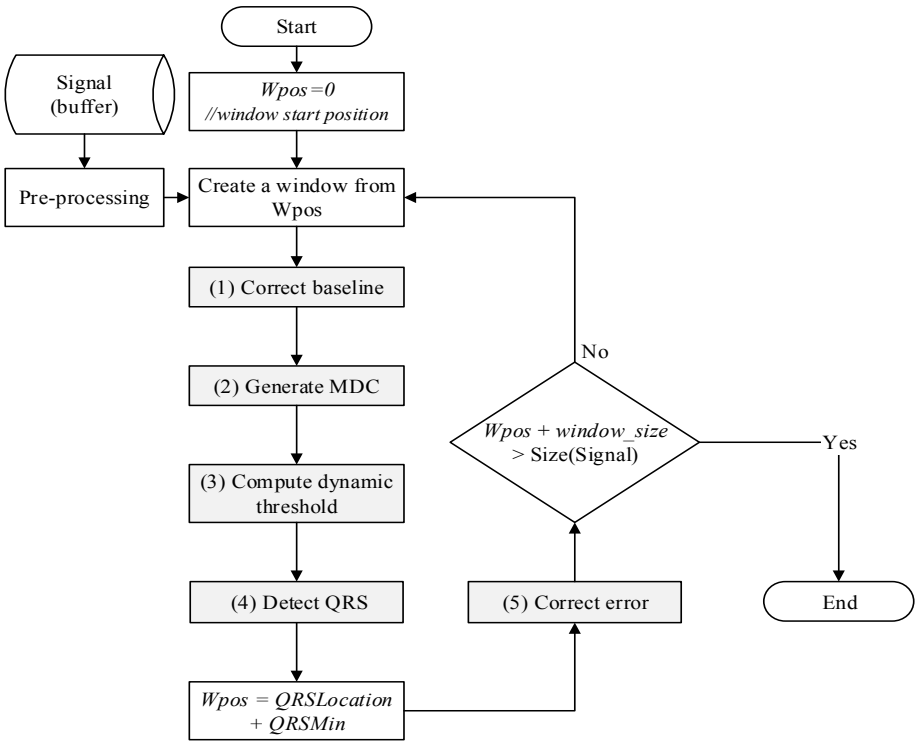

Fig. 3 - A flowchart of the proposed sliding window-based method (*Wpos* denotes the starting position of the window)

Therefore, the proposed algorithm consists of five key steps: baseline correction (Section 3.1.1), MMD curve generation (Section 3.1.2), dynamic threshold computation (Section 3.1.3), R-peak detection (Section 3.1.4), and error correction (Section 3.1.5). The flowchart of the proposed method is illustrated in Fig. 3. Each key step is discussed in detail, as follows.

Before applying the proposed MMD algorithm, a sliding window average filtering strategy is first used to filter the major spikes, since they highly affect the peak detection process. Eq. (1) is used to perform the operation.

$$y_c(x) = \begin{cases} \frac{1}{w}\sum_{i=1}^{w} y\left(x + i - \frac{w}{2}\right) & \text{If } \frac{w}{2} \le x \le size(y) - \frac{w}{2} \\ y(x) & Otherwise \end{cases} \quad (1)$$

where $w = round(fs \times 0.02) + round(fs \times 0.02)\%2$

Note that $y(x)$ indicates the amplitude of the raw ECG signal at sample x; $y_c(x)$ represents the filtered output signal at sample x; $size(y)$ represents the length of the raw ECG signal, y; i denotes the index of the sliding window; fs indicates the sampling frequency of the signal; w represents the filtering window size, which is an even number close to the number of samples in 0.02 second; symbol '%' indicates the modulo operation, which returns the remainder after dividing one number with another.

3.1.1. Baseline Correction

Baseline wander occurs frequently in ECG readings, especially when mobile ECG sensors are used. In this research, baseline wander is removed by subtracting the local average of the signal from the raw signal. Eq. (2) is used to perform the operation.

$$y_b(x) = \begin{cases} y(x) - \frac{1}{w}\sum_{i=1}^{w} y\left(x + i - \frac{w}{2}\right) & If\ \frac{w}{2} \le x \le size(y) - \frac{w}{2} \\ y(x) & Otherwise \end{cases} \quad (2)$$

where $w = round(fs \times 0.5) + round(fs \times 0.5)\%2$

Note that *y(x)* indicates the raw ECG signal; $y_b(x)$ denotes the baseline corrected signal; while the window length *w* is an even number close to the number of samples in half a second. Fig. 4 shows an example of the ECG signal with baseline wander (top) and the corrected signal (bottom). Again, symbol '%' indicates the modulo operation, which returns the remainder after dividing one number with another.

3.1.2. Max-Min Difference Curve Generation

The Max-Min Difference Curve (MDC) represents the difference between the highest and lowest amplitudes in a window region. Eqs. (3) and (4) are used for MDC generation:

$$y_{mdc}(x) = Max(W(x)) - Min(W(x)) \tag{3}$$

$$W(x) = \begin{cases} \left\{y\left(x+1-\frac{w}{2}\right), \dots, y\left(x+w-\frac{w}{2}\right)\right\} & If \ \frac{w}{2} \le x \le size(y) - \frac{w}{2} \\ \{y(1), \dots, y(w)\} & Else\ if \ x < \frac{w}{2} \\ \{y(size(y)-w+1), \dots, y(size(y))\} & Otherwise \end{cases} \tag{4}$$

where $w = round(fs \times 0.14) + round(fs \times 0.14)\%2$

Note that *W(x)* represents local window at position *x*; the window size *w* is an even number, close to the number of samples in 0.14 seconds, since most of the QRS complex fits in this length [44]. Fig. 5 illustrates an example of MDC along with the ECG signal. It is noticeable that all peaks in the MDC are positive, and are aligned to the QRS complexes of the corresponding ECG signal.

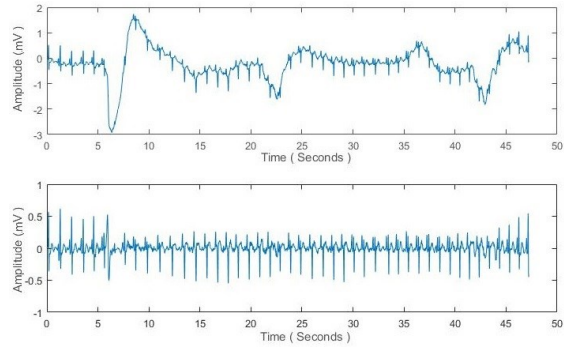

Fig. 4 – An example ECG signal with baseline wander (top) and the corrected ECG signal (bottom)

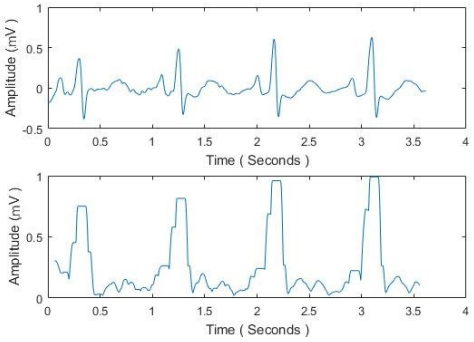

Fig. 5 - An example ECG signal (top) and the corresponding MDC (bottom)

3.1.3. Dynamic Threshold Computation

As explained earlier, not all peak values in the MDC represent the R-peaks in actual ECG signals. An inappropriate threshold could lead to errors in treating a P or T wave as an R wave. The threshold for R-peak detection not only varies from time to time, but also from signal to signal. Here, we employ two decision making parameters to determine the subsequent occurrence of the QRS complex, i.e., the location threshold (*tLoc*) and the amplitude threshold (*tAmp*). There are three key procedures: initialisation; updating; and time varying threshold selection. We first initialize the variables required for threshold calculation. Then, the threshold is updated in each iteration according to its previous values. After that, it is finalised based on the current position and other factors. The details of these three procedures are described, as follows.

- ***Initialization***

We first set *tLoc* = 0.2×*fs,* since the maximum heartbeat per minute can only reach up to 300 (i.e., 0.2 second per heartbeat). Then, *tAmp* is initialized as *pf*×*max(W(x))* for the first iteration, where *W*(*x*) is the search window; *pf* is the peak factor representing the minimum factor of previous peaks to be taken as the next threshold. Considering that the number of heartbeat per minute cannot be lower than 24 (or 2.5 second per heartbeat) and an QRS complex stays for 0.14 second only [44], a fixed window size, *w,* is defined, as follows:

$$w = round(fs \times 2.64) + round(fs \times 2.64)\%2 \tag{5}$$

As mentioned earlier, we assume that the maximum duration for a single heartbeat is no longer than 2.5 second. Combining an additional QRS length of 0.14 second, we initialize the window to the closest even number equivalent size of 2.64 second of the signal. This setting ensures that the window includes at least one heartbeat.

The start point of the search window, *ws*, is initialized as follows.

$$ws = rLoc + round(fs \times 0.14) \tag{6}$$

where *rLoc* is the location of the current R-peak. The next search window skips the current QRS region, as our algorithm detects the start of QRS. Therefore, when the R wave is missing, we skip for a duration of 0.14 second (i.e., the standard QRS duration).

- ***Updating***

After the first *n* iterations, *tAmp* and *tLoc* are updated according to the previous values of *mAmp* and *mLoc* using Eqs. (7) and (8), respectively.

$$tAmp(x) = \frac{1}{n+1}\left(\sum_{i=1}^{n} mAmp(x-i) + mAmp(x)\right) \tag{7}$$

$$tLoc(x) = \frac{1}{2}\left(\frac{1}{n-1}\left(mLoc(x-1) - mLoc(x-n)\right)\right) \tag{8}$$

where *n* is the recall number representing the number of previous QRS properties to remember; *mAmp*(*x*) and *mLoc*(*x*) are the amplitude and location of the selected peak above the threshold of the MDC at iteration *x,* respectively.

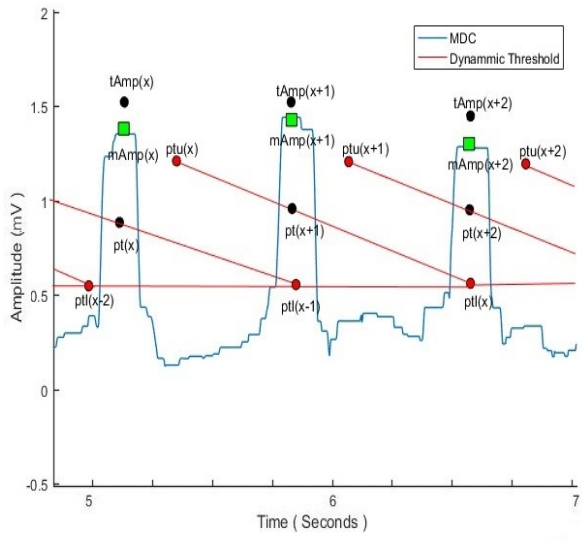

Fig. 6 - Time varying dynamic threshold selection with respect to the MDC

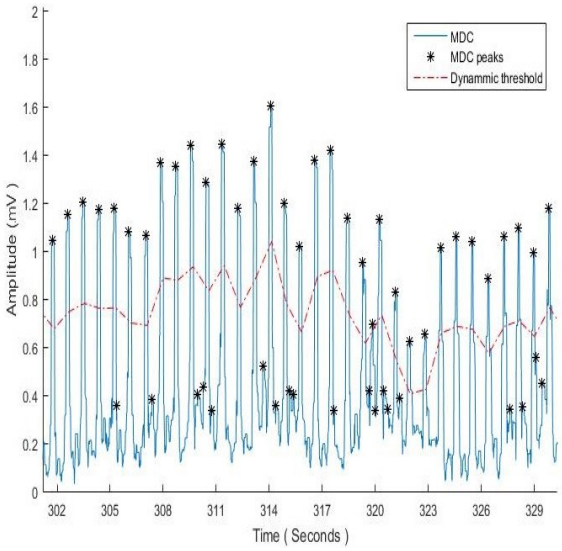

Fig. 7 - MDC and dynamic thresholds

- ***Time varying threshold selection***

Subsequently, depending on the position of the current peak, we determine the threshold value. We use linear interpolation of values between an upper threshold (*ptu*) and a lower threshold (*ptl*) based on the distance between the current peak and previously detected QRS location. After one MDC peak is selected as an R peak, we update *ptu*(*x*) and *ptl*(*x*) using Eqs. (9) and (10) respectively.

$$ptu(x) = tAmp(x) \times uf \tag{9}$$

$$ptl(x) = tAmp(x) \times lf \tag{10}$$

We calculate the peak threshold $pt(x)$ for the current peak x using Eq. (11), as follows:

$$pt(x) = \begin{cases} ptu(x) + \big(ptl(x) - ptu(x)\big) \times \dfrac{mLoc(x) - \ rLoc(last) - 0.14fs}{2tLoc(x) - rLoc(last) - 0.14fs} & If\ mLoc(x) - rLoc(last) \ < \ 2 \times tLoc(x) \\ ptl(x) & Otherwise \end{cases} \quad (11)$$

where $rLoc(last)$ denotes the last detected R-peak location.

An example of how the proposed dynamic thresholding works is shown in Fig. 6. Considering its x^{th} peak, $ptu(x)$ and $ptl(x)$ are calculated using Eqs (9) and (10), respectively as discussed earlier. The next search window starts from the location of $ptu(x)$, which is $rLoc(last)+0.14\times fs$. Depending on the distance between the last QRS location and the location of the current peak on the MDC, we vary the peak threshold from $ptu(x)$ to $ptl(x)$. If it is more than twice of the average R-R distance, or $2\times tLoc(x)$, we fix the threshold at $ptl(x)$. When the next peak is selected, we update the values and repeat the same process. In Fig. 6, we illustrate the details of this dynamic thresholding mechanism. The red lines represent the hypothetical thresholds connecting *ptu* and *ptl*. Only one point on the line is selected as the peak threshold, *pt,* depending on the occurrence of the peak on the MDC. Fig. 7 shows an example of the MDC along with those selected thresholds (*pt*), which are connected to form a dotted red line.

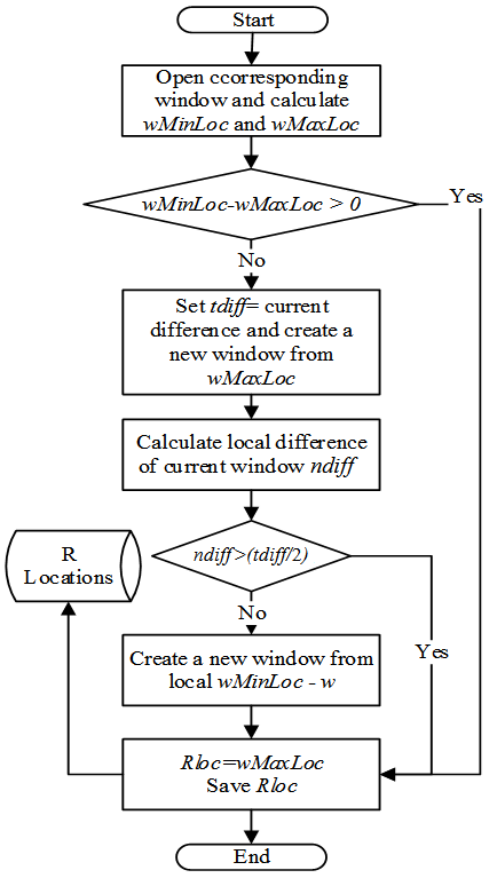

wMaxLoc: the maximum amplitude location in the local window.
wMinLoc: the minimum amplitude location in the local window.
tdiff: the temporary difference between the local minimum and maximum amplitudes.
ndiff: the difference between the local minimum and maximum amplitudes.
w: the window size.
Rloc: the location of the R wave

Fig. 8 - Flowchart of R detection from the MDC peak

3.1.4. R-Peak Detection

The MDC peak is either selected or discarded depending on the threshold calculated earlier. The proposed algorithm creates a window of MDC starting from *ws* with a width of *w*. After that, the following steps are performed.

- Firstly, the local maxima are detected, which have an amplitude larger than $pt(x)$, and are stored as $mAmp(x)$ along with location $mLoc(x)$.

- *If* $mLoc(x) - mLoc(x-1) <= round(fs \times 0.14)$ and $mAmp(x) > mAmp(x-1)$, we discard the previous R location, and continue with the current iteration x.
- After the peaks are detected on the MDC, we process the actual signal to obtain the R-peak location.

Fig. 8 depicts a flowchart for finding the R location from the MDC peak, *mLoc*. The pseudo codes are presented in Algorithm 1.

Algorithm 1: R-Peak Detection
Input:
mLoc //Location of the peak found on the MDC
Y(x) //The original ECG signal
Output:
rLoc //Location of the R wave if present, otherwise, the location of the Q wave.
Begin
{
window=W(*mLoc*); //Create a window
start=*mLoc*;
[*wMin*, *wMinLoc*]= min(window); //Find the value and location of the minimum point in the window
[*wMax*, *wMaxLoc*]= max(window); //Find the value and location of the maximum point in the window
If *wMinLoc*-*wMaxLoc*<0 **then** //If the minimum point occurs before the maximum point, the maximum could be R or T wave
    tdiff=*wMax*-*wMin*; //Save the maximum-minimum difference
    new_window=W(start+*wMaxLoc*); //Create a new window from the maximum location
    start=start+*wMaxLoc*; //Update the start point of the window
    [*wMin*, *wMinLoc*]=min(new_window); //Find the value and location of the minimum point in the new window
    [*wMax*, *wMaxLoc*]=max(new_window); //Find the value and location of the maximum point in the new window
    ndiff=*wMax*-*wMin*; //Calculate the maximum-minimum difference
    If *ndiff*<*tdiff*/2 **then** //If the new difference is less than half of the previous difference
        new_window=W(start+*wMinLoc*-*w*) //Create a new window before the current window
        start= start+*wMinLoc*-*w* //Update the start point of window
        [~, *wMaxLoc*]= max(new_window); //Find the location of the maximum point in the new window
    Endif
Endif
rLoc = start + *wMaxLoc* //Save the location of the maximum point
Output *rLoc*
}
End

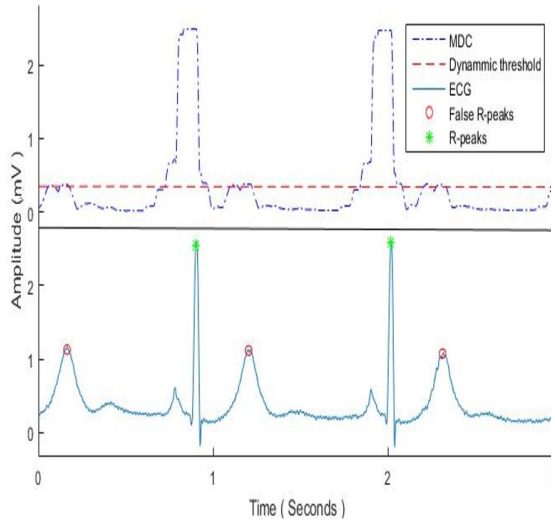

Fig. 9 - The MDC with an inefficient upper threshold (top) and R-peak detection results shown on the ECG signal (bottom)

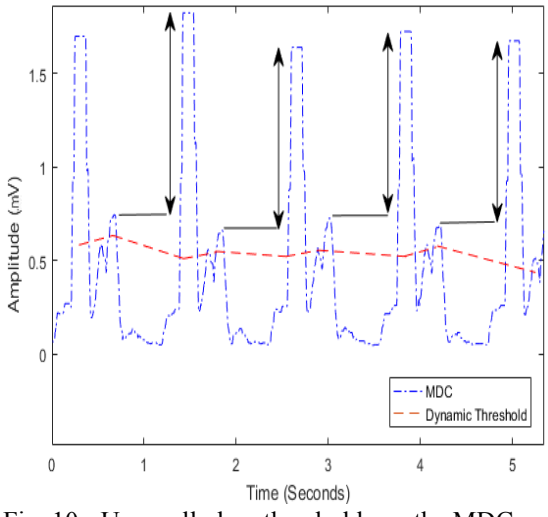

Fig. 10 - Unusually low thresholds on the MDC

3.1.5. Error Correction

False positive errors are detected, which are mainly caused by large T waves or a low initial upper threshold for R-peak detection. Fig. 9 shows an example of unusually low thresholds on the MDC, leading to false positive R-peak detection. The top diagram in Fig. 9 shows the MDC with a low threshold, and the signal below is the corresponding ECG with false positive beat markers. Therefore, we use the following procedure to discard the falsely detected T waves and adjust the upper threshold accordingly.

Firstly, we compute the last n differences of the detected R-peak amplitude pairs. The resulting amplitudes, which are marked with double arrows in Fig. 10, are calculated using Equation (12). In Fig. 10, a sequence of alternating higher and lower peaks above the dynamic threshold line can be observed explicitly. Such a situation is only possible if the T peaks have been mistakenly detected as the R peaks continuously. Therefore, in this step, we calculate the difference between multiple consecutive peak pairs using Equation (12).

$$k(i)= rAmp(x\text{-}(i\text{-}1)\times 2)\text{-}R(x\text{-}(i\text{-}1)\times 2\text{-}1) \tag{12}$$

The above calculation is repeated until we have at least $n\times 2$ elements in $rAmp$.

- Check if the inequalities, $absolute(k(i))>0.25\times rAmp(x\text{-}(i\text{-}1)\times 2)$ and $absolute(k(i)\text{-}k(i\text{-}1))<0.25\times rAmp(x\text{-}(i\text{-}1)\times 2)$, hold for all $i=[1,2,..(n\text{-}1)]$. We then discard the lower R location in each pair, and update uf using Eq. (13).

$$uf = uf + \frac{1}{2} absolute\left(\frac{k(1)}{tAmp(x)}\right) \tag{13}$$

In our experimental study, we employ three pairs of R amplitudes for error correction (i.e., i = 1, 2, and 3) and for adjustment of the upper R threshold factor (uf).

Although the abovementioned error correction operation usually does not affect ECG signals with normal T waves, this process is particularly useful for reducing false positives for those signals where the T waves are sufficiently large. As an example, ECG signals with considerably large T waves are observed in MITDB, e.g. signals 113, 117, 200, 215, 217. These signals generate more false positive results in the absence of the abovementioned error correction procedure. To demonstrate this claim, we initialize n=5 and execute our algorithm using signal 113 from MITDB. The outcomes are 393 false positives and 0 false positive without and with the error correction procedure, respectively, indicating efficiency of the proposed error correction procedure.

Furthermore, we employ the following strategy for performance evaluation of the proposed MMD algorithm. The QRS detection results consist of true positive (*TP*), false positive (*FP*), and false negative (*FN*). *TP* represents the total number of QRS complexes that have been accurately identified; *FP* represents the total number of QRS complexes that have been falsely marked even though they are not actually QRS complexes; *FN* represents the total number of QRS complexes that have not been identified at all. We use sensitivity (*SN*) and positive predictivity (*PP*) for evaluation of QRS detection, as shown in Eqs (14) and (15), respectively. *SN* represents the percentage of correctly detected heartbeats, while *PP* represents the percentage of detected heartbeats that are actually true. The detailed evaluation results for QRS detection are presented and discussed in Section 4.

$$SN = \frac{TP}{TP + FN} \times 100\% \tag{14}$$

$$PP = \frac{TP}{TP + FP} \times 100\% \tag{15}$$

3.2. Detection of the Locations of P, Q, S and T Waves

To further demonstrate the potential of the proposed MMD algorithm for abnormality detection in ECG signals, we detect the locations of P, Q, S, and T waves based on the detected R-peak locations. Algorithm 2 (in Appendix) shows the peak detection procedure for P, Q, S and T waves without compromising computational efficiency. The algorithm employs a local extrema search process to identify the locations of P, Q, S and T peaks for abnormality detection. The search process finds the local minima and maxima. The algorithm takes a raw ECG signal and the R-peak location as the inputs, and provides the estimated peak locations of P, Q, S, and

T waves as the outputs. Although more complex processing for peak detection of P, Q, S and T waves is available [45, 46], some of them tend to be computationally expensive. The detection of each wave (e.g. P or T wave) also constitutes a research topic on its own [47, 48]. In this research, we employ a comparatively lightweight peak detection algorithm (i.e., Algorithm 2) for detection of P, Q, S and T waves. The results indicate that it is efficient in accurately recovering the locations of P, Q, S and T waves, without distracting the focus of the research on the proposed MMD algorithm for QRS detection too much. Moreover, only the signals with accurate QRS detection are employed in this step for peak detection of P, Q, S, and T waves and for subsequent abnormality analysis.

3.3. Feature Extraction and Neural Network Classification

After recovering the peak locations of P, Q, S, and T waves, we further generate a total of 16 customised features for abnormality detection. Fig. 11 lists these 16 features, where features 1 to 11 are marked with dotted lines. Features 1 to 5 represent the normalized distances of P-peak R-peak, Q-peak R-peak, R-peak S-peak, Q-peak S-peak and R-peak T-peak, respectively. Features 6 to 10 indicate the amplitudes of P, Q, R, S, and T waves from the baseline. Feature 11 is the normalized distance between the current and subsequent R-peak locations. Features 12 to 16 (marked as shaded areas in Figure 11) represent the areas between P, Q, R, S, and T waves and the baseline, respectively. The detailed calculations of these features are summarized in Table 1. The empirical results indicate the efficiency of the above extracted features, which have also been employed in our previous research for abnormality detection from ECG signals [49].

A feedforward artificial neural network classifier, i.e., the multilayer perceptron [50], is subsequently used for abnormal heartbeat detection. The abovementioned 16 features form the inputs. The classifier employs the backpropagation algorithm as the learning mechanism [50]. To achieve the best trade-off between classification accuracy and computational efficiency, after several trials, the network structure is set to: 16 nodes in the input layer (each handles one of the 16 extracted features), 10 nodes in the hidden layer, and 2 nodes in the output layer (represent the normal and abnormal classes). The detailed evaluation results and discussion are presented in Section 4.

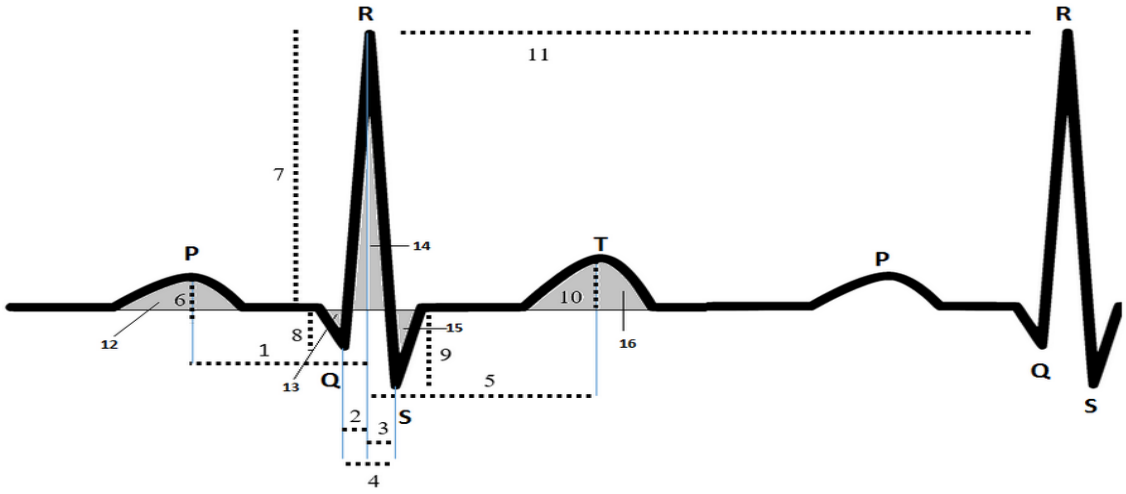

Fig. 11 - The extracted 16 features for abnormality detection

Table 1: Definition of the extracted 16 features

No.	Expression	Description
1	(*locR – locP*)*/fs*	Normalized P-peak R-peak distance.
2	(*locR – locQ*)*/fs*	Normalized Q-peak R-peak distance.
3	(*locS – locR*)*/fs*	Normalized R-peak S-peak distance.
4	(*locS – locQ*)*/fs*	Normalized Q-peak S-peak distance.
5	(*locT – locR*)*/fs*	Normalized R-peak T-peak distance.
6	*ampP – ampB*	P-peak amplitude (where *ampB* refers to the baseline amplitude of the signal).
7	*ampR – ampB*	R-peak amplitude.
8	*ampB – ampQ*	Q-peak amplitude.
9	*ampB – ampS*	S-peak amplitude.

10	$ampT - ampB$	T-peak amplitude.
11	$(locR_{after}\text{-}locR)/fs$	Normalized distance between two adjacent R-peaks
12	$\sum_{i=locP-kp}^{locP+kp} \mid y(i) - ampB(i) \mid /fs$	Area of P wave (where *kp* is half of the average P wave duration and $y(i)$ is the i^{th} sample of the original signal).
13	$\sum_{i=locQ-kq}^{locQ+kq} \mid ampB(i) - y(i) \mid /fs$	Area of Q wave (where *kq* is half of the average Q wave duration).
14	$\sum_{i=locR-kr}^{locR+kr} \mid y(i) - ampB(i) \mid /fs$	Area of R wave (where *kr* is half of the average R wave duration).
15	$\sum_{i=locS-ks}^{locS+ks} \mid ampB(i) - y(i) \mid /fs$	Area of S wave (where *ks* is half of the average S wave duration).
16	$\sum_{i=locT-kt}^{locT+kt} \mid y(i) - ampB(i) \mid /fs$	Area of T wave (where *kt* is half of the average T wave duration).

4. Results

In this section, an empirical evaluation for QRS detection and abnormality identification to ascertain the efficiency of the proposed MMD algorithm and its potential for disease detection using multiple ECG databases is presented. A performance comparison between our work and other related studies is included.

4.1. Experimental Data

We employed raw single lead ECG data samples extracted from five different databases in the PhysioNet [51] databank for evaluation. The test databases employed were the MIT-BIH Arrhythmia Database (MITDB) [2], the European ST-T Database (EDB) [3], the MIT-BIH ST Change Database (STDB) [4], the St.-Petersburg Institute of Cardiological Technics 12-lead Arrhythmia Database (INCARTDB) [5] and the QT Database (QTDB) [6]. We used the first lead (i.e., Lead II) from each ECG recording for evaluation in this study.

4.2. Evaluation Results

4.2.1. QRS Detection

We carried out the first set of experiments with the MIT-BIH Arrhythmia database [2]. Table 2 shows the signal-wise detailed results of multiple algorithms including Pan and Tompkins algorithm [37], Wavelet transform method by Li *et al*. [52], difference operation method by Wang *et al*. [12], and the JQRS method [53, 54]. The window with a fixed size of 80 ms around the R peak is considered as true positive for the MIT-BIH Arrhythmia database. This is because in the MIT-BIH Arrhythmia database, the S wave is marked as the QRS location when the R wave is missing, while our algorithm marks the Q position as the QRS location under the same situation.

As illustrated in Table 2, our proposed algorithm is comparable with other related state-of-the-art algorithms reported in the literature for R-peak detection. Our algorithm works very efficiently, except for Signals 105 and 207, where it yields some false positive results due to noise. True positive is calculated based on a tolerance window of 80 ms for all the algorithms, in order to have a fair comparison. Our proposed algorithm works not only for normal heartbeats but also for those with abnormalities. Examples of some abnormalities extracted from the MIT-BIH Arrhythmia database along with the detected R-peaks by our algorithm are depicted in Fig. 12. As indicated in Fig. 12, in most cases, our algorithm correctly identifies the QRS locations owing to the use of the MMD (i.e., the regional difference between the minimum and maximum amplitudes), which remains the highest on the QRS locations (as evidenced in Fig. 2 (b)) for all these cases.

Moreover, we compared the proposed MMD algorithm with the most recent state-of-the-art JQRS method using five databases for QRS detection. Overall, a set of 1,232,138 heartbeats from five different databases was used for evaluation. The detailed comparison between our algorithm and the JQRS method is shown in Table 3. Our algorithm achieves an overall average sensitivity of 99.62% and an average positive predictivity of 99.67%, and outperforms the JQRS method consistently. Our results pertaining to QTDB show a very low false positive rate, leading to an overall highest positive predictivity of 99.91%. In addition, the performances of both our algorithm and the JQRS method pertaining to INCARTDB are comparatively low, due to the fact that the signals in INCARTDB contain more noise and are less enhanced as compared with those in QTDB and STDB.

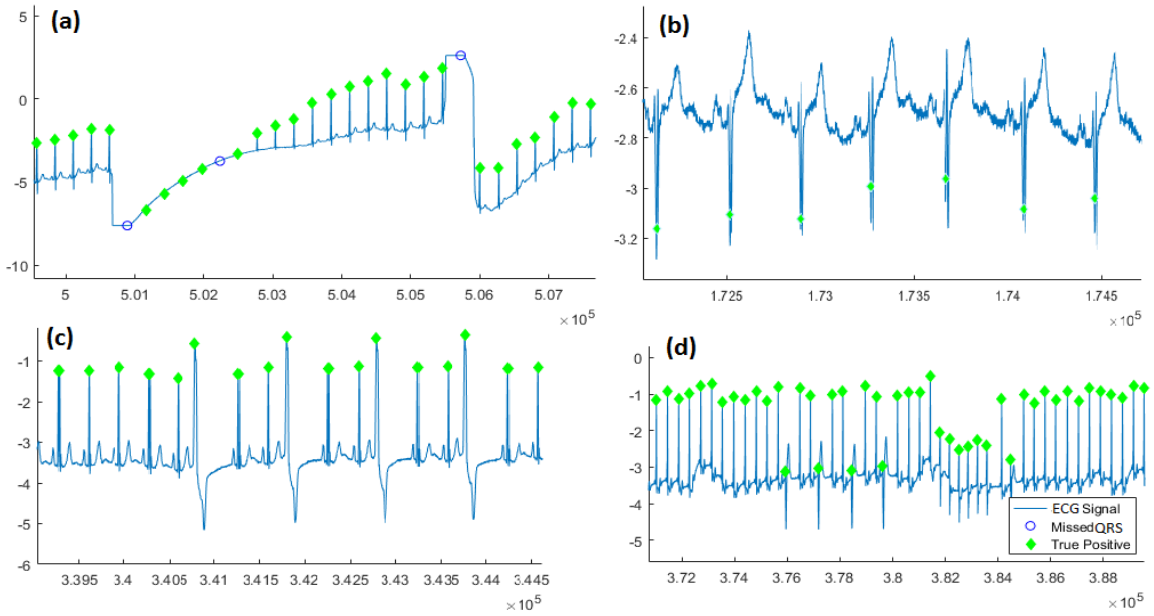

Fig. 12 - Examples of abnormal signals extracted from the MIT-BIH Arrhythmia database with the corresponding QRS positions detected by the proposed algorithm. These abnormal signals include (a) a poor quality signal due to noise interference; (b) premature ventricular contraction beats; (c) premature ventricular contraction combined with normal heartbeats; (d) right bundle branch block beats, with the *x* axis representing samples of the raw signals and the *y* axis indicating the signal amplitude in mV.

We also compared our algorithm with some related methods described in Elgendi *et al*. [23] for R-peak detection, as shown in Table 4. Since most of these related methods employ the MITDB database for evaluation, we present the results for the same database for comparison. The proposed algorithm achieves comparable performance using lightweight methods, at a fraction of latency and resource demands.

Table 3: Comparison between the proposed MMD algorithm and the JQRS method

Database	# beats	MMD					JQRS [53, 54]				
		TP	FP	FN	*SN*	*PP*	TP	FP	FN	*SN*	*PP*
MITDB	109809	109432	369	389	99.65	99.66	108571	412	923	99.16	99.62
EDB	790495	788746	2208	1749	99.78	99.72	787953	2608	2612	99.67	99.67
STDB	70755	70696	170	59	99.92	99.76	70373	385	407	99.42	99.46
INCRDB	174644	172276	1205	2368	98.64	99.31	157547	6999	18355	89.57	95.75
QTDB	86435	86320	78	115	99.87	99.91	86409	118	584	99.33	99.86
Total	1232138	1227470	4030	4680	99.62	99.67	1210853	10522	22881	98.15	99.14

Table 4: Performance comparison with related methods for R-peak detection

Publication	Methodologies	Beats	*SN*	*PP*
Pan and Tompkins [37]	Bandpass filter + first derivative + squaring + moving average + multiple thresholds	116137	99.76	99.56
Li *et al*. [52]	Wavelet transform + digital filter + singularity + thresholds	104182	98.89	99.94
Afonso *et al*. [25]	Filter bank + thresholds	90909	99.59	99.56
Benitez *et al*. [22]	First derivative + Hilbert transform + threshold	109257	99.13	99.31
Moraes *et al*. [55]	Low pass filter + first derivative + modified spatial velocity + threshold	109481	99.69	99.88

Christov [39]	Multiple moving averages + first derivative + thresholds	109494	99.76	99.81
Martinez *et al*. [10]	Wavelet transform + Multiple thresholds + zero Crossing	109428	99.8	99.86
Chiarugi *et al*. [38]	Bandpass filter + first Derivative + thresholds	109494	99.76	99.81
Arzeno *et al*. [56]	First derivative + Hilbert transform + thresholds	109517	99.68	99.63
Wang *et al*. [12]	Bandpass Filter + Difference Operation + thresholds	108517	99.86	99.95
Chouhan *et al*. [57]	Digital filters + threshold	102654	99.55	99.49
Elgendi *et al*. [58]	Digital filters + thresholds	44677	97.50	99.90
Ghaffari *et al*. [59]	Continuous Wavelet transform + threshold	109837	99.91	99.72
Zheng and Wu [20]	Discrete Wavelet transform + Cubic Spline Interpolation + moving average + threshold	N/R	98.68	99.59
Elgendi [40]	Bandpass filter + first derivative + squaring + thresholding using two moving averages	109985	99.78	99.87
Chouakri *et al.* [18]	Wavelet transform + histogram + moving average + two thresholds	109488	98.68	97.24
Zidelmal *et al.* [60]	Wavelet transform + coefficients multiplication + two thresholds	109494	99.64	99.82
Rodríguez *et al*. [15]	Bandpass filter + first Derivative + Fast Fourier transform + adaptive threshold	44715	96.28	99.71
The proposed approach	Moving average filter + dynamic thresholding + MMC generation	109809	99.65	99.66

4.2.2. Abnormality Detection

Integrated with a feature extraction technique and a neural network classifier, the proposed MMD algorithm was extended for normal and abnormal heartbeat detection. The MITDB database was employed for abnormality detection. We combined all types of abnormality annotations in this database as a single abnormal class. Overall, we used 37492 normal and 34414 abnormal heartbeats for evaluation using 10-fold cross validation. Table 5 summarises the experimental results.

Table 5: Confusion matrix for the classification results of normal/abnormal heartbeat detection

	True Normal	True Abnormal	Class Precision
Predicted Normal	95.50%	8.80%	91.50%
Predicted Abnormal	4.50%	91.20%	94.52%
Class Recall	93.86%	92.40%	Overall Accuracy
Total	37492 heartbeats	34414 heartbeats	93.44%

As shown in Table 5, the proposed MMD algorithm combined with a lightweight feature extraction technique and neural network classifier yields an accuracy rate of 93.44% for abnormality detection. The empirical results further indicate the superiority and efficiency of the proposed MMD algorithm for abnormal heartbeat detection. In future work, we aim to employ more complex processing techniques for P, Q, S and T peak detection in order to achieve further improvement.

4.2.3. Complexity Evaluation

We further demonstrated computational efficiency of the proposed algorithm in comparison with other related methods, i.e., JQRS [53, 54] and the algorithm of Pan and Tompkins [37], for R-peak detection. The computational cost was based on experiments conducted using MATLAB on a PC with 2.5 GHz CPU. Four databases, i.e., MITDB, EDB, STDB, and INCERTDB, were employed for evaluation. For a comparison, the related QRS detection methods such as JQRS [53, 54] and Pan and Tompkins [37], along with our proposed algorithm were all implemented in MATLAB. The same test databases shown in Table 6 were used for evaluation.

We applied the JQRS method [53, 54] and the algorithm of Pan and Tompkins [37] on a 5-second sliding window to each signal from the test databases for comparison of computational efficiency. Note that these conventional methods [53, 54, 37] were not designed for sliding window based analysis. Table 6 shows the

computational costs. Comparatively, these conventional methods not only have higher computational costs but also produce a comparatively larger number of false positive results for R-peak detection. This could be due to the fact that these conventional methods were not designed for sliding window based analysis, and might require the entire ECG signal for analysis, in order to obtain a good frequency resolution as opposed to a small sliding window-based processing approach. On the contrary, the proposed MMD algorithm obtains optimal computational efficiency and shows great robustness in dealing with real-time QRS detection with impressive performance. Overall, its computational complexity is at the order of $O(n)$, where n is the length of an ECG signal.

Table 6: Comparison of the average CPU time elapsed (in seconds) for R-peak detection

Databases	JQRS [53, 54]	Pan and Tompkins [37]	The proposed MMD algorithm
MITDB	19.1097	12.12012	10.23568
EDB	42.12465	34.51354	31.64323
STDB	14.32272	10.4369	9.578125
INCERTDB	10.79729	8.016667	7.815833

5. Discussion

In this research, we propose a sliding window-based MMD algorithm for robust real-time R-peak detection from raw single lead ECG signals. In comparison to other R-peak detection algorithms, the proposed MMD algorithm has a low computational cost. Evaluated with five well-known databases, the proposed algorithm outperforms other state-of-the-art methods, such as JQRS, consistently. Some theoretical comparison between the proposed MMD algorithm and other related research is conducted below.

As the state-of-the-art methods, JQRS [53, 54] and the algorithm of Pan and Tompkins [37] have been widely used for QRS complex detection. The algorithm of Pan and Tompkins [37] includes the following procedures, i.e., resampling, mean subtraction, bandpass filter, differentiation, squaring, moving-window integration and a complex dual-thresholding process. However, some of the above processes, such as resampling, bandpass filtering, and dual-thresholding, require high computational costs and memory resources.

JQRS [53, 54] embeds a window-based peak energy detector. Instead of using the bandpass filter, it employs a QRS matched filter for pre-processing. It also uses heuristic and search-back strategies to deal with flat lines and missed beats, respectively**.** Although JQRS is more complex in comparison with the proposed MMD algorithm, it is not designed for sliding window based analysis and may require the entire ECG signals for R-peak detection analysis in order to obtain reliable competitive detection accuracy.

Rodríguez *et al.* [15] implemented a QRS detector which includes the processing of bandpass filter, differentiation, Hilbert transform and adaptive thresholding, whereas Li *et al.* [52] employed wavelet transforms for R-peak detection. Although both wavelet and Hilbert transforms are effective techniques for time-frequency analysis and are capable of characterizing the local regularity of signals, both techniques are computationally costly and inefficient for real-time ECG analysis compared with the proposed method.

Elgendi [40] employed an optimized knowledge-based QRS detector which included three stages, i.e., pre-processing (bandpass filter and squaring), generating blocks of interest and thresholding. The decision-making of the last two steps was also supported by a knowledge base. Their work was motivated by the assumption that a QRS detector employing the prior knowledge of the ECG features was inclined to possess better performances. However, their algorithm requires a time-consuming brute-force search based optimization process beforehand to identify complex optimal parameter settings.

In comparison with the above R-peak detection methods, this research proposes a novel MMD algorithm with dynamic thresholding for robust QRS detection. Instead of requiring the whole signal to be stored in memory, it employs a sliding window-based strategy and uses a small buffer of the signal for online real-time ECG analysis. In order to further ascertain the usefulness of the proposed MMD algorithm, it has been further extended for abnormal/normal heartbeat detection with the integration of a feature extraction technique and a neural network classifier. The empirical results indicate that the proposed algorithm shows great superiority over other methods in terms of R-peak detection accuracy and computational efficiency.

6. Conclusions

We have proposed the MMD algorithm for QRS detection based on single lead (mostly Lead II) ECG signals in this study. It consists of five key steps, namely baseline correction, Max-Min Difference curve generation, dynamic threshold computation, QRS detection, and error correction. The main contribution of the proposed MMD algorithm is its lightweight real-time QRS detection scheme without compromising detection accuracy. The proposed MMD algorithm is useful to provide accurate QRS detection from diverse cross-domain ECG

signals with efficient computational complexity. Evaluated using five well-known databases, the proposed MMD algorithm achieves impressive performances in comparison with those from other related models for R-peak detection using both normal and abnormal ECG signals. Integrated with a feature extraction technique and a neural network classifier, the proposed MMD algorithm has been further extended for abnormal/normal heartbeat detection. The empirical results indicate the efficiency and superiority of the proposed MMD algorithm for abnormality detection. However, its performance degrades when noisy signals, especially with high amplitude spikes, are used.

For further work, we will conduct a comprehensive investigation to overcome the noise problem. We will also extend the proposed algorithm to undertake more complex heart disease detection problems, e.g. the obtained R-R interval results can be used directly for determining R-R interval related heart abnormality. In addition, the proposed algorithm can be integrated with more complex mobile ECG feature extraction algorithms to find the base position of a heartbeat for a detailed analysis to determine the P and T wave positions along with their durations and shapes. Ultimately, we aim to embed the proposed algorithm into mobile devices as a base QRS detector to promote early detection of heart diseases.

Acknowledgement

This research is supported by the European Union (EU) sponsored (Erasmus Mundus) cLINK (Centre of excellence for Learning, Innovation, Networking and Knowledge) project (EU Grant No. 2645).

REFERENCES

[1] S. Gradl, P. Kugler, C. Lohmuller, B. Eskofier, Real-time ECG monitoring and arrhythmia detection using Android-based mobile devices, in: Proceedings of the Annual International Conference of the IEEE Engineering in Medicine and Biology Society, EMBS, IEEE, 2012: pp. 2452–2455. doi:10.1109/EMBC.2012.6346460.

[2] G.B. Moody, R.G. Mark, The impact of the MIT-BIH arrhythmia database, IEEE Engineering in Medicine and Biology Magazine. 20 (2001) 45–50. doi:10.1109/51.932724.

[3] A. Taddei, G. Distante, M. Emdin, P. Pisani, G.B. Moody, C. Zeelenberg, C. Marchesi, The European ST-T database: standard for evaluating systems for the analysis of ST-T changes in ambulatory electrocardiography, European Heart Journal. 13 (1992) 1164–72. http://www.ncbi.nlm.nih.gov/pubmed/1396824 (accessed 22 February 2016).

[4] P. Albrecht, ST segment characterization for long term automated ECG analysis, M.S. thesis, MIT Dept. of Electrical Engineering and Computer Science, 1983.

[5] St.-Petersburg Institute of Cardiological Technics 12-lead Arrhythmia Database, https://physionet.org/pn3/incartdb/. (2016). https://physionet.org/pn3/incartdb/ (accessed 24 April 2016).

[6] P. Laguna, R.G. Mark, A. Goldberg, G.B. Moody, A database for evaluation of algorithms for measurement of QT and other waveform intervals in the ECG, in: Computers in Cardiology 1997, 1997: pp. 673–676. doi:10.1109/CIC.1997.648140.

[7] E.D. Übeyli, Implementing Wavelet Transform mixture of experts network for analysis of electrocardiogram beats, Expert Systems. 25 (2008) 150–162. doi:10.1111/j.1468-0394.2008.00444.x.

[8] J.P.V. Madeiro, P.C. Cortez, J.A.L. Marques, C.R.V. Seisdedos, C.R.M.R. Sobrinho, An innovative approach of QRS segmentation based on first-derivative, Hilbert and Wavelet Transforms, Medical Engineering and Physics. 34 (2012) 1236–1246. doi:10.1016/j.medengphy.2011.12.011.

[9] T. Pan, L. Zhang, S. Zhou, Detection of ECG characteristic points using biorthogonal spline Wavelet, in: 2010 3rd International Conference on Biomedical Engineering and Informatics, IEEE, 2010: pp. 858–863. doi:10.1109/BMEI.2010.5639905.

[10] J.P. Martenez, R. Almeida, S. Olmos, A.P. Rocha, P. Laguna, A Wavelet-based ECG delineator evaluation on standard databases, IEEE Transactions on Biomedical Engineering. 51 (2004) 570–581. doi:10.1109/TBME.2003.821031.

[11] H. Zhou, Real-time automatic ECG diagnosis method dedicated to pervasive cardiac care, Wireless Sensor Network. 1 (2009) 276–283. doi:10.4236/wsn.2009.14034.

[12] W.J. Wang, Y.C. Yeh, QRS complexes detection for ECG signal: The Difference Operation Method, Computer Methods and Programs in Biomedicine. 91 (2008) 245–254. doi:10.1016/j.cmpb.2008.04.006.

[13] E.D. Ubeyli, Feature extraction for analysis of ECG signals, in: Annual International Conference of the IEEE Engineering in Medicine and Biology Society, 2008: pp. 1080–1083. doi:10.1109/IEMBS.2008.4649347.

[14] T. Alkhaldi, L. Mihaylova, H. Gellersen, QRS complex detection using centered cumulative sums of squares, in: Signal Processing: Algorithms, Architectures, Arrangements, and Applications (SPA), IEEE, 2013: pp. 168–171.

[15] R. Rodríguez, A. Mexicano, J. Bila, S. Cervantes, R. Ponce, Feature extraction of Electrocardiogram signals by applying Adaptive Threshold and Principal Component Analysis, Journal of Applied Research and Technology. 13 (2015) 261–269. doi:10.1016/j.jart.2015.06.008.

[16] H. Gothwal, S. Kedawat, R. Kumar, Cardiac arrhythmias detection in an ECG beat signal using fast fourier transform and artificial neural network, Journal of Biomedical Science and Engineering. 4 (2011) 289–296. doi:10.4236/jbise.2011.44039.

[17] X. Xu, Y. Liu, Adaptive threshold for QRS complex fetection based on Wavelet Transform, Annual International Conference of the IEEE Engineering in Medicine and Biology Society. 7 (2005) 7281–4. doi:10.1109/IEMBS.2005.1616192.

[18] S.A. Chouakri, F. Bereksi-Reguig, A. Taleb-Ahmed, QRS complex detection based on multi Wavelet packet decomposition, Applied Mathematics and Computation. 217 (2011) 9508–9525. doi:10.1016/j.amc.2011.03.001.

[19] E.M. Tamil, N.H. Kamarudin, R. Salleh, M.Y.I. Idris, M. Noor, A.M. Tamil, Heartbeat Electrocardiogram (ECG) signal feature extraction using Discrete Wavelet Transforms (DWT), in: CSPA (2008), 2008: pp. 1112–1117.

[20] H. Zheng, J. Wu, Real-time QRS detection method, in: HealthCom 2008 - 10th International Conference on E-Health Networking, Applications and Services, 2008: pp. 169–170. doi:10.1109/HEALTH.2008.4600130.

[21] D. Benitez, P.A. Gaydecki, A. Zaidi, A.P. Fitzpatrick, The use of the Hilbert transform in ECG signal analysis, Computers in Biology and Medicine. 31 (2001) 399–406. doi:10.1016/S0010-4825(01)00009-9.

[22] D.S. Benitez, P.A. Gaydecki, A. Zaidi, A.P. Fitzpatrick, A new QRS detection algorithm based on the Hilbert Transform, in: Computers in Cardiology 2000, 2000: pp. 379–382. doi:10.1109/CIC.2000.898536.

[23] M. Elgendi, B. Eskofier, S. Dokos, D. Abbott, Revisiting QRS detection methodologies for portable, wearable, battery-operated, and wireless ECG systems, PLoS ONE. 9 (2014) e84018. doi:10.1371/journal.pone.0084018.

[24] J. Lee, K. Jeong, J. Yoon, M. Lee, A simple real-time QRS detection algorithm, in: 18th Annual International Conference of the IEEE Engineering in Medicine and Biology Society, IEEE, 1996: pp. 1396–1398. doi:10.1109/IEMBS.1996.647473.

[25] V.X. Afonso, O. Wieben, W.J. Tompkins, T.Q. Nguyen, Filter bank-based ECG beat classification, in: 19th Annual International Conference of the IEEE Engineering in Medicine and Biology Society., IEEE, 1997: pp. 97–100. doi:10.1109/IEMBS.1997.754474.

[26] P.-C. Hii, W.-Y. Chung, A comprehensive ubiquitous healthcare solution on an Android™ mobile device, Sensors (Basel). 11 (2011) 6799–6815. doi:10.3390/s110706799.

[27] P.O. Borjesson, O. Pahlm, L. Sornmo, M.-E. Nygards, Adaptive QRS detection based on maximum a posteriori estimation, IEEE Transactions on Biomedical Engineering. BME-29 (1982) 341–351. doi:10.1109/TBME.1982.324901.

[28] Q. Xue, Y.H. Hu, W.J. Tompkins, Neural-Network-based adaptive matched filtering for QRS detection, IEEE Transactions on Biomedical Engineering. 39 (1992) 317–329. doi:10.1109/10.126604.

[29] G. Vijaya, V. Kumar, H.K. Verma, ANN-based QRS-complex analysis of ECG, Journal of Medical Engineering & Technology. 22 (1998) 160–7. doi:10.3109/03091909809032534.

[30] Y.H. Hu, W.J. Tompkins, J.L. Urrusti, V.X. Afonso, Applications of Artificial Neural Networks for ECG signal detection and classification, Journal of Electrocardiology. 26 Suppl (1993) 66–73. http://www.ncbi.nlm.nih.gov/pubmed/8189150.

[31] M.G. Strintzis, G. Stalidis, X. Magnisalis, N. Maglaveras, Use of Neural Networks for Electrocarciogram (ECG) feature extraction, recognition and classification, Neural Network World Journal. 3 (1992) 313–328.

[32] S. Dobbs, N. Schmitt, H. Ozemek, QRS detection by template matching using real-time correlation on a microcomputer, Journal of Clinical Engineering. 9 (1984) 197–212. http://journals.lww.com/jcejournal/Abstract/1984/07000/QRS_Detection_By_Template_Matching_Using_Real_Time.2.aspx (accessed 22 February 2016).

[33] D. Ebenezer, V. Krishnamurthy, Wave digital matched filter for electrocardiogram preprocessing, Journal of Biomedical Engineering. 15 (1993) 132–134. doi:10.1016/0141-5425(93)90042-W.

[34] M. Ayat, M.B. Shamsollahi, B. Mozaffari, S. Kharabian, ECG denoising using modulus maxima of wavelet transform, Proceedings of the 31st Annual International Conference of the IEEE Engineering in Medicine and Biology Society: Engineering the Future of Biomedicine, EMBC 2009. 2009 (2009) 416–419. doi:10.1109/IEMBS.2009.5332617.

[35] C. Hennig, R. Orglmeister, QRS detection using Zero Crossing Counts, Progress in Biomedical Research. 8 (2003) 138–145. http://progress.biomed.uni-erlangen.de/documents/200308030138.pdf (accessed 22 February 2016).

[36] O. Adeluyi, J. Lee, R-READER : A lightweight algorithm for rapid detection of ECG signal R-peaks, in: International Conference on Engineering and Industries (ICEI) 2011, IEEE, 2011: pp. 1–5.

[37] J. Pan, W.J. Tompkins, A real-time QRS detection algorithm, IEEE Transactions on Bio-Medical Engineering. 32 (1985) 230–236. doi:10.1109/TBME.1985.325532.

[38] F. Chiarugi, V. Sakkalis, D. Emmanouilidou, T. Krontiris, M. Varanini, I. Tollis, Adaptive threshold QRS detector with best channel selection based on a noise rating system, in: Computers in Cardiology, 2007: pp. 157–160. doi:10.1109/CIC.2007.4745445.

[39] I.I. Christov, Real time electrocardiogram QRS detection using combined adaptive threshold, Biomedical Engineering Online. 3 (2004) 28. doi:10.1186/1475-925X-3-28.

[40] M. Elgendi, Fast QRS detection with an optimized knowledge-based method: evaluation on 11 standard ECG databases, PLoS

ONE. 8 (2013) e73557. doi:10.1371/journal.pone.0073557.

[41] F. Miao, Y. Cheng, Y. He, Q. He, Y. Li, A wearable context-aware ECG monitoring system integrated with built-in kinematic sensors of the smartphone, Sensors (Switzerland). 15 (2015) 11465–11484. doi:10.3390/s150511465.

[42] A. Rehman, M. Mustafa, I. Israr, M. Yaqoob, Survey of wearable sensors with comparative study of noise reduction ECG filters, International Journal of Computing and Network Technology. 1 (2013) 61–81. doi:10.12785/ijcnt/010105.

[43] Y. Wang, S. Doleschel, R. Wunderlich, S. Heinen, A wearable wireless ECG monitoring system with dynamic transmission power control for long-term homecare, Journal of Medical Systems. 39 (2015) 35. doi:10.1007/s10916-015-0223-5.

[44] R.M. Rangayyan, Biomedical signal analysis: a case-study approach, Annals of Biomedical Engineering. 30 (2002) 552. doi:10.1002/9780470544204.

[45] C. Lin, C. Mailhes, J.Y. Tourneret, P- and T-wave delineation in ECG signals using a bayesian approach and a partially collapsed gibbs sampler, IEEE Transactions on Biomedical Engineering. 57 (2010) 2840–2849. doi:10.1109/TBME.2010.2076809.

[46] M. Rahimpour, B. Mohammadzadeh Asl, P wave detection in ECG signals using an extended Kalman filter: an evaluation in different arrhythmia contexts, Physiological Measurement. 37 (2016) 1089–1104. doi:10.1088/0967-3334/37/7/1089.

[47] M.B. Messaoud, B. Khelil, A. Kachouri, Analysis and parameter extraction of P wave using correlation method, International Arab Journal of Information Technology (IAJIT). 6 (2009) 40–46.

[48] M. Elgendi, B. Eskofier, D. Abbott, Fast T wave detection calibrated by clinical knowledge with annotation of P and T waves, Sensors (Basel). 15 (2015) 17693–17714. doi:10.3390/s150717693.

[49] D. Pandit, L. Zhang, N. Aslam, C. Liu, S. Chattopadhyay, Improved abnormality detection from raw ECG signals using feature enhancement, in: The 2016 12th International Conference on Natural Computation, Fuzzy Systems and Knowledge Discovery (ICNC-FSKD 2016), IEEE, 2016: p. (in press).

[50] J. Han, M. Kamber, J. Pei. Data mining: concepts and techniques, 3rd edn, Morgan Kaufmann, (2011).

[51] A.L. Goldberger, L.A.N. Amaral, L. Glass, J.M. Hausdorff, P.C. Ivanov, R.G. Mark, J.E. Mietus, G.B. Moody, C.-K. Peng, H.. Stanley, PhysioBank, PhysioToolkit, and PhysioNet: components of a new research resource for complex physiologic signals, Circulation. 101 (2000) 215–220. doi:10.1161/01.CIR.101.23.e215.

[52] C. Li, C. Zheng, T. Changfeng, Detection of ECG characteristic points using Wavelet transforms, IEEE Transactions on Biomedical Engineering. 42 (1995) 21–28. doi:10.1109/10.362922.

[53] A.E.W. Johnson, J. Behar, F. Andreotti, G.D. Clifford, J. Oster, Multimodal heart beat detection using signal quality indices, Physiological Measurement. 36 (2015) 1665–77. doi:10.1088/0967-3334/36/8/1665.

[54] J. Behar, J. Oster, G.D. Clifford, Combining and benchmarking methods of foetal ECG extraction without maternal or scalp electrode data, Physiological Measurement. 35 (2014) 1569–1589. doi:10.1088/0967-3334/35/8/1569.

[55] J. Moraes, M.M. Freitas, F.N. Vilani, E.V. Costa, A QRS complex detection algorithm using electrocardiogram leads, in: Computers in Cardiology, 2002: pp. 205–208. doi:10.1109/CIC.2002.1166743.

[56] N.M. Arzeno, Z.D. Deng, C.S. Poon, Analysis of first-derivative based QRS detection algorithms, IEEE Transactions on Biomedical Engineering. 55 (2008) 478–484. doi:10.1109/TBME.2007.912658.

[57] V.S. Chouhan, S.S. Mehta, Detection of QRS complexes in 12-lead ECG using adaptive quantized threshold, International Journal of Computer Science and Network Security. 8 (2008) 155–163.

[58] M. Elgendi, S. Mahalingam, M. Jonkman, F.D. Boer, A robust QRS complex detection algorithm using dynamic thresholds, in: International Symposium on Computer Science and Its Applications, 2008: pp. 153–158. doi:10.1109/CSA.2008.16.

[59] A. Ghaffari, H. Golbayani, M. Ghasemi, A new mathematical based QRS detector using continuous Wavelet Transform, Computers & Electrical Engineering. 34 (2008) 81–91. doi:10.1016/j.compeleceng.2007.10.005.

[60] Z. Zidelmal, A. Amirou, M. Adnane, A. Belouchrani, QRS detection based on Wavelet coefficients, Computer Methods and Programs in Biomedicine. 107 (2012) 490–496. doi:10.1016/j.cmpb.2011.12.004.

Table 2: Performance comparison between MMD and other QRS detection algorithms on MIT-BIH arrhythmia database

Signal	# beats	MMD (proposed)				Pan and Tompkins [37]				Wang *et al.* [12]				Li *et al.* [52]				JQRS [53, 54]			
		FP	FN	*SN*	*PP*	FP	FN	*SN*	*PP*	FP	FN	*SN*	*PP*	FP	FN	*SN*	*PP*	FP	FN	*SN*	*PP*
100	2273	0	2	99.91	100.00	0	0	100.00	100.00	0	1	99.96	100.00	0	0	100.00	100.00	0	0	100.00	100.00
101	1865	0	0	100.00	100.00	5	3	99.84	99.73	0	1	99.95	100.00	1	0	100.00	99.95	4	1	99.95	99.79
102	2187	0	0	100.00	100.00	0	0	100.00	100.00	0	1	99.95	100.00	0	0	100.00	100.00	0	1	99.95	100.00
103	2084	0	2	99.90	100.00	0	0	100.00	100.00	0	0	100.00	100.00	0	0	100.00	100.00	0	5	99.76	100.00
104	2230	3	3	99.87	99.87	1	0	100.00	99.96	2	0	100.00	99.91	8	2	99.91	99.64	13	23	98.97	99.41
105	2572	73	4	99.84	97.16	67	22	99.13	97.40	0	17	99.34	100.00	15	13	99.49	99.42	27	2	99.92	98.96
106	2027	0	19	99.07	100.00	5	2	99.90	99.75	0	6	99.70	100.00	2	3	99.85	99.90	0	65	96.79	100.00
107	2137	0	71	96.78	100.00	0	2	99.91	100.00	0	3	99.86	100.00	0	0	100.00	100.00	0	2	99.91	100.00
108	1763	13	3	99.83	99.26	199	22	98.61	88.71	6	0	100.00	99.66	13	15	99.15	99.26	27	7	99.60	98.49
109	2532	0	1	99.96	100.00	0	1	99.96	100.00	0	3	99.88	100.00	0	0	100.00	100.00	0	9	99.64	100.00
111	2124	0	1	99.95	100.00	1	0	100.00	99.95	0	1	99.95	100.00	1	1	99.95	99.95	0	2	99.91	100.00
112	2539	2	0	100.00	99.92	0	1	99.96	100.00	1	0	100.00	99.96	2	1	99.96	99.92	0	0	100.00	100.00
113	1795	0	2	99.89	100.00	0	0	100.00	100.00	9	0	100.00	99.50	2	0	100.00	99.89	0	0	100.00	100.00
114	1879	4	1	99.95	99.79	3	17	99.10	99.84	0	1	99.95	100.00	3	0	100.00	99.84	3	7	99.63	99.84
115	1953	0	2	99.90	100.00	0	0	100.00	100.00	0	0	100.00	100.00	0	0	100.00	100.00	0	0	100.00	100.00
116	2412	3	16	99.34	99.88	3	22	99.10	99.88	0	17	99.30	100.00	0	1	99.96	100.00	2	24	99.00	99.92
117	1535	1	0	100.00	99.93	1	1	99.93	99.93	2	0	100.00	99.87	1	0	100.00	99.93	0	0	100.00	100.00
118	2275	0	0	100.00	100.00	1	0	100.00	99.96	10	0	100.00	99.56	1	0	100.00	99.96	0	0	100.00	100.00
119	1987	0	0	100.00	100.00	1	0	100.00	99.95	0	0	100.00	100.00	1	0	100.00	99.95	0	2	99.90	100.00
121	1863	1	2	99.89	99.95	4	7	99.62	99.79	0	2	99.89	100.00	2	1	99.95	99.89	0	1	99.95	100.00
122	2476	0	0	100.00	100.00	1	1	99.96	99.96	0	0	100.00	100.00	0	0	100.00	100.00	0	1	99.96	100.00
123	1518	0	0	100.00	100.00	0	0	100.00	100.00	0	0	100.00	100.00	0	0	100.00	100.00	0	3	99.80	100.00
124	1619	0	0	100.00	100.00	0	0	100.00	100.00	1	0	100.00	99.94	0	0	100.00	100.00	0	11	99.32	100.00
200	2601	1	4	99.85	99.96	6	3	99.88	99.77	5	0	100.00	99.81	0	1	99.96	100.00	2	3	99.88	99.92
201	1963	0	51	97.47	100.00	0	10	99.49	100.00	0	20	98.99	100.00	1	12	99.39	99.95	0	67	96.59	100.00
202	2136	0	3	99.86	100.00	0	4	99.81	100.00	1	0	100.00	99.95	0	1	99.95	100.00	0	11	99.49	100.00
203	2982	12	66	97.83	99.60	53	30	98.99	98.22	16	2	99.93	99.46	2	24	99.20	99.93	10	60	97.99	99.66
205	2656	0	6	99.77	100.00	0	2	99.92	100.00	0	16	99.40	100.00	0	1	99.96	100.00	0	7	99.74	100.00
207	1862	224	10	99.39	87.97	4	4	99.79	99.79	0	1	99.95	100.00	2	3	99.84	99.89	303	57	96.94	85.61
208	2956	4	29	99.03	99.86	4	14	99.53	99.86	0	14	99.53	100.00	0	4	99.86	100.00	3	438	85.18	99.88
209	3004	3	0	100.00	99.90	3	0	100.00	99.90	1	0	100.00	99.97	0	0	100.00	100.00	1	0	100.00	99.97
210	2647	3	40	98.51	99.89	2	8	99.70	99.92	0	14	99.47	100.00	3	3	99.89	99.89	3	35	98.68	99.89
212	2748	0	0	100.00	100.00	0	0	100.00	100.00	1	0	100.00	99.96	0	0	100.00	100.00	0	0	100.00	100.00
213	3251	0	5	99.85	100.00	1	2	99.94	99.97	0	3	99.91	100.00	0	0	100.00	100.00	0	6	99.82	100.00
214	2262	0	4	99.82	100.00	2	4	99.82	99.91	0	4	99.82	100.00	–	–	–	–	0	10	99.56	100.00
215	3363	0	2	99.94	100.00	0	1	99.97	100.00	0	4	99.88	100.00	–	–	–	–	0	2	99.94	100.00
217	2208	0	6	99.73	100.00	4	6	99.73	99.82	0	2	99.91	100.00	1	1	99.95	99.95	0	6	99.73	100.00
219	2154	0	0	100.00	100.00	0	0	100.00	100.00	0	0	100.00	100.00	0	0	100.00	100.00	0	3	99.86	100.00
220	2048	0	0	100.00	100.00	0	0	100.00	100.00	0	0	100.00	100.00	0	0	100.00	100.00	0	0	100.00	100.00
221	2427	0	0	100.00	100.00	2	0	100.00	99.92	0	1	99.96	100.00	0	7	99.71	100.00	0	16	99.34	100.00
222	2484	1	6	99.76	99.96	101	81	96.71	95.93	0	5	99.80	100.00	1	9	99.64	99.96	1	6	99.76	99.96
223	2605	0	2	99.92	100.00	1	0	100.00	99.96	1	0	100.00	99.96	0	2	99.92	100.00	0	6	99.77	100.00
228	2053	19	19	99.07	99.07	25	5	99.75	98.78	0	2	99.90	100.00	3	7	99.66	99.85	11	4	99.81	99.47
230	2256	0	0	100.00	100.00	1	0	100.00	99.96	2	0	100.00	99.91	0	0	100.00	100.00	0	0	100.00	100.00
231	1886	0	0	100.00	100.00	0	0	100.00	100.00	0	15	99.21	100.00	0	0	100.00	100.00	0	0	100.00	100.00
232	1780	2	0	100.00	99.89	6	1	99.94	99.66	0	0	100.00	100.00	0	0	100.00	100.00	2	0	100.00	99.89
233	3079	0	7	99.77	100.00	0	1	99.97	100.00	0	9	99.71	100.00	0	0	100.00	100.00	0	16	99.48	100.00
234	2753	0	0	100.00	100.00	0	0	100.00	100.00	0	1	99.96	100.00	0	0	100.00	100.00	0	4	99.85	100.00

Appendix

Algorithm 2: Peak detection for P, Q, S and T waves from each detected R wave

Input:

Y(x) //The original ECG signal
locR //Location of R
qrsT //QRS distance threshold
pT //P distance threshold
tT //T distance threshold

Output:

locP //Location of the P
locQ //Location of the Q
locS //Location of the S
locT //Location of the T
ampP //Amplitude of the P
ampQ //Amplitude of the Q
ampS //Amplitude of the S
ampT //Amplitude of the T

Begin

//Search the left-hand side of the R location for the minimum value within the half QRS distance threshold range
locQ = location of minimum in *Y(locR - Round(qrsT/2) : locR);*
//Search the right-hand side of the R location for the minimum value within the half QRS distance threshold range
locS = location of minimum in *Y(locR : locR + Round(qrsT/2));*
//Search the left-hand side of the Q location for the maximum value within the P distance threshold range
locP = location of maximum in *Y(Q - pT : locQ);*
//Search the right-hand side of the S location for the maximum value within the T distance threshold range
locT = location of maximum in *Y(S : tT);*
ampQ = Y(locQ);
ampS = Y(locS);
amp = Y(locP);
ampT = Y(locT);

End